Application of the "k_{obs}" method for the study of tight-binding reversible inhibitors

Petr Kuzmič

BioKin Ltd., Watertown, Massachusetts 02472, USA

Abstract

The mathematics and geometry of the "k_{obs}" method under the tight-binding experimental conditions, when inhibitor depletion is significant, has not been fully explored in the existing biochemical kinetic literature. It is shown here that under tight-binding conditions a plot of the pseudo-first order rate constant against the inhibitor concentration is always nonlinear and concave upward, as opposed to either linear or hyperbolic (concave downward) in the absence of inhibitor depletion. If and when the apparent inhibition constant is lower than the active enzyme concentration, the plot has a distinct local minimum occurring at an inhibitor concentration that is equal to the enzyme concentration minus the inhibition constant. The slope of the plot at inhibitor concentrations significantly higher than the enzyme concentration is equal to the second order bimolecular association rate constant. The intercept on the vertical axis is equal to the sum of the dissociation rate constant of the enzyme–inhibitor complex, plus the product of the enzyme concentration multiplied by the association rate constant. Most importantly, we show here that specifically under tight-binding experimental conditions the "k_{obs}" method only applies to the one-step binding model, without a possible involvement of a transient enzyme–inhibitor complex. Thus, as a matter of principle, under tight binding this method cannot be used to discriminate between the one-step and two-step inhibition mechanisms, nor can it be used to determine the dissociation equilibrium of a transient complex even if such a complex is in fact present.

Key words:
enzyme kinetics; inhibition; tight-binding; mathematics; statistics; rate equation

1. Introduction

The "k_{obs}" method in reversible enzyme inhibition kinetics consists of analyzing the reaction time-course in two consecutive steps. In the first phase of the data analysis, each individual kinetic trace is analyzed separately to determine an apparent first-order rate constant using an appropriate algebraic model for the reaction progress. In the second step, the values of apparent first-order rate constants so determined are fit to another algebraic model, which is based on a presumed mechanism of inhibition. For example, depending on the exact nature of the mathematical relationship between k_{obs} and the inhibitor concentration $[\text{I}]_0$, it might be possible to determine whether or not the enzyme–inhibitor interaction proceeds with an involvement of a transient intermediate.

Textbook literature on the kinetic evaluation of enzyme inhibitors [1] contains certain simple algebraic formulas (see below) that can be used to determine the number of microscopic inhibition steps and the values of relevant kinetic constants from k_{obs} data. Those formulas are applicable to simplified experimental conditions without the involvement of tight-binding, i.e., without inhibitor depletion [2, 3]. An important complication arises when the inhibition assay is in fact conducted under tight-binding experimental conditions, where at least some inhibitor concentrations already causing a measurable inhibitory effect are comparable with the enzyme concentration.

This report describes a data-analytic method that can be used to determine, under tight-binding experimental conditions, not only the association and dissociation rate constants for an reversible enzyme inhibitor but – in certain favorable cases – simultaneously also the active enzyme concentration from relevant k_{obs} data. Importantly, it is clarified here that the classical formulas for the dependence of k_{obs} on the total inhibitor concentration cannot and should not be used to determine the number steps appearing in the inhibition mechanism under tight-binding experimental conditions. Nor can those formulas be used, specifically under tight-binding conditions, to determine the dissociation equilibrium constant of a transient enzyme–inhibitor complex even if such a complex is in fact present.

2. Theory

This section reviews previously published theoretical results and also presents a detailed analysis of those results specifically as they pertain to the k_{obs} method.
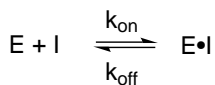
2.1. Algebraic models for inhibition time-course

We will be considering two kinetic mechanisms of enzyme inhibition shown in *Scheme 1*. In the single-step Mechanism **A**, the enzyme and inhibitor reversibly form a single noncovalent complex; k_{on} is the association rate constant and k_{off} is the dissociation rate constant. The two-step Mechanism **B** involves a rapid (effectively instantaneous) formation of an initial complex, which relatively slowly rearranges into a final complex;
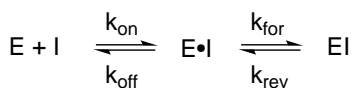

Email: `petr.kuzmic@gmail.com` (Petr Kuzmič)

k_{for} is the forward isomerization rate constant and k_{rev} is the reverse isomerization rate constant.

Mechanism **A**:

$$E + I \underset{k_{off}}{\overset{k_{on}}{\rightleftharpoons}} E \bullet I$$

Mechanism **B**:

$$E + I \underset{k_{off}}{\overset{k_{on}}{\rightleftharpoons}} E \bullet I \underset{k_{rev}}{\overset{k_{for}}{\rightleftharpoons}} EI$$

rapid equilibrium: $K_d = k_{off} / k_{on}$

Scheme 1

Note that the substrate branch of the overall catalytic mechanisms is absent in *Scheme 1*. Consequently, in the theoretical analysis below all references to the bimolecular association rate constant k_{on} should be interpreted as meaning the *apparent* second-order association rate constant k_{on}^* according to the formulas previously derived by Cha [4] for the apparent inhibition constants [3].

2.1.1. Algebraic model in the absence of inhibitor depletion

The algebraic formalism discussed in this report assumes throughout that in the absence of inhibitors the time course of the enzyme assay is strictly linear, in the sense that the reaction rate effectively does not change over time. In the simplified case of zero inhibitor depletion, i.e., in the absence of tight binding, Cha [4] has shown that the time course of an inhibition assay is described by Eqn (1), where F is some observable experimental signal such as fluorescence; F_0 is the baseline instrument offset; v_0 is the initial reaction rate; v_s is the reaction rate at steady state; t is the reaction time; and k_{obs} is the apparent first-order rate constants. Note that unlike the closely related Eqn. (34) in Cha's original report [4], the reaction rates v_0 and v_s appearing in Eqn (1) are expressed in instrument units (e.g., fluorescence units per second) as opposed to in concentration units (e.g., micromoles of product formed per minute).

$$F = F_0 + v_s t + \frac{v_0 - v_s}{k_{obs}} \left[1 - \exp(-k_{obs} t)\right] \quad (1)$$

$$k_{obs} = k_{off} + k_{on}[I]_0 \qquad \text{mechanism } \mathbf{A} \quad (2)$$

$$k_{obs} = k_{rev} + k_{for} \frac{[I]_0}{[I]_0 + K_d} \qquad \text{mechanism } \mathbf{B} \quad (3)$$

Cha [4, Table 1] has also shown that in the absence of inhibitor depletion Eqns (2)–(3) can be used to diagnose how many steps appear in the inhibition mechanism. In particular, if the plot of k_{obs} data vs. the inhibitor concentration $[I]_0$ is distinctly hyperbolic, we can conclude there is an involvement of a intermediate complex. (Note however that, unlike the classic Michaelis-Menten type saturation curve, the hyperbola defined

by Eqn (3) does *not* go through the origin of the coordinate system.) In contrast, a strictly linear plot of k_{obs} vs. $[I]_0$ suggests that the inhibitor and enzyme associate in a single step. In that case the slope of the linear plot is identical to the association rate constant k_{on} and the intercept is identical to the dissociation rate constant k_{off}.

2.1.2. Algebraic model in the presence of inhibitor depletion

Under tight-binding experimental conditions inhibitor depletion is significant, in the sense that the mole fraction of the inhibitor bound to the enzyme cannot be neglected in the inhibitor's mass balance. Under these particular experimental circumstances, Williams *et al.* [5] have shown that the time course of the enzyme assay is described by Eqn (4), where γ is an auxiliary variable defined by Eqn (5).

$$F = F_0 + v_s t + \frac{v_0 - v_s}{k_{obs}} \frac{1 - \gamma}{\gamma} \ln \frac{1 - \gamma \exp(-k_{obs} t)}{1 - \gamma} \quad (4)$$

$$\gamma = \frac{[E]_0}{[I]_0} \left(1 - \frac{v_s}{v_0}\right)^2 \quad (5)$$

$$k_{obs} = k_{on} \sqrt{\left([E]_0 - [I]_0 - \frac{k_{off}}{k_{on}}\right)^2 + 4[E]_0 \frac{k_{off}}{k_{on}}} \quad (6)$$

Importantly, Eqns (4)–(5) can only be applied to the one-step Mechanism **A**, in which case the apparent rate constant k_{obs} depends on the inhibitor and enzyme concentrations as is shown in Eqn (6) (see Eqn. (5) in the original paper [5]). Williams *at al.* [5] have demonstrated that, specifically under tight-binding experimental conditions, it is theoretically impossible to derive any closed-form algebraic formula for the reaction progress under the two-step Mechanism **B**, similar to Eqn (4). According to these authors, the only possible way to obtain a mathematical model for the reaction progress under tight-binding conditions following Mechanism **B** is to perform a *numerical integration* of a relevant system of first-order ordinary differential equations (ODEs). Thus, it is fundamentally impossible to differentiate between the one-step Mechanism **A** and the two-steps Mechanism **B** on the basis of k_{obs} data derived from the tight-binding rate Eqn (4), which only applies to the one-step binding mechanism.

2.2. Mathematical properties of the "tight-binding" k_{obs} rate constant

Enzymologists involved in the study of enzyme inhibition under classical (as opposed to tight-binding) experimental conditions are accustomed to viewing and analyzing plots of k_{obs} against the inhibitor concentration $[I]_0$, in an effort to discern the number of binding steps involved in the inhibition mechanism. A strictly linear plot normally signifies a one-step binding model, whereas a hyperbolic plot (with an nonzero offset on the Y-axis) signifies a two-step binding model. Under tight-binding experimental conditions, when k_{obs} values are derived

from Eqn (4), it is impossible to discern the number of binding steps from the shape of the plot. Nevertheless visualizing the expected shape of such plots might prove illuminating. An illustrative example is shown in *Figure 1*.
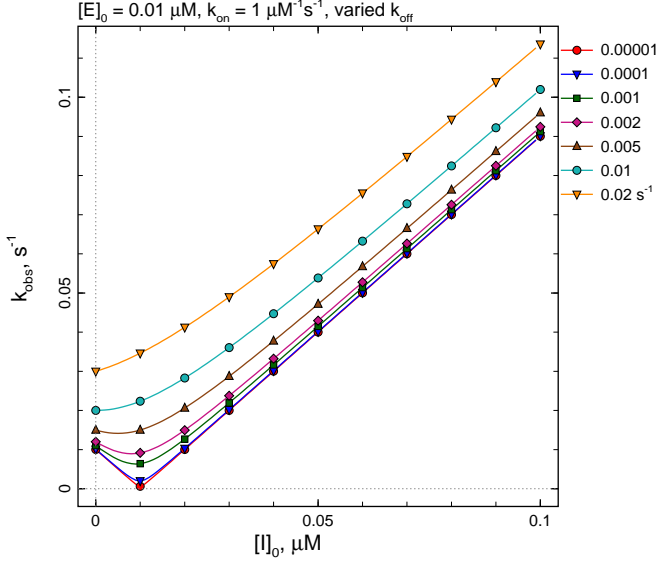
Figure 1: Expected shapes of the k_{obs} vs. $[I]_0$ plot under the tight-binding experimental conditions. For explanation see text.

The overall shape of the k_{obs} vs. $[I]_0$ plot under tight-binding conditions is always ever-so-slightly concave upward. In some cases, depending on the value of $K_i = k_{off}/k_{on}$, there is a prominent minimum. In fact, at extremely low values of K_i, the minimum on the plot corresponds to zero k_{obs} value occurring at exactly $[I]_0 = [E]_0$. At sufficiently high inhibitor concentrations the k_{obs} plot appears linear with a slope that does not depend on the K_i but only on the association rate constant k_{on}.

$$\frac{dk_{obs}}{d[I]_0} = -k_{on}\frac{[E]_0 - [I]_0 - K_i}{\sqrt{([E]_0 - [I]_0 - K_i)^2 + 4[E]_0 K_i}} \qquad (7)$$

To understand these qualitative feature better, we can differentiate Eqn (6) with respect to $[I]_0$ to obtain Eqn (7), which represents the slope of the k_{obs} plot. Setting the left-hand side of Eqn (7) to zero and solving for $[I]_0$, we can determine that there is a minimum on the k_{obs} curve at $[I]_0 = [E]_0 - K_i$. However, a distinct minimum is observable on the positive $[I]_0$ half-axis only if $K_i < [E]_0$. Setting $[I]_0 \gg [E]_0$ and $[I]_0 \gg K_i$ in Eqn (7) we can also discover that the asymptotic slope of the tight-binding k_{obs} plot is equal to k_{on}, as in the classical binding situation represented by Eqn (2).

The intercept on the vertical k_{obs} axis can be found by setting $[I]_0 = 0$ in Eqn (6) and simplifying the resulting square root expression to obtain $k_{obs} = k_{off} + k_{on}[E]_0$. Note that under classical, as opposed to tight-binding, experimental conditions the intercept on the vertical axis is at $k_{obs} = k_{off}$, according to Eqn (2). In other words, tight binding simply shifts the Y-axis intercept upward by $k_{on}[E]_0$.

It should be noted that under tight-binding conditions k_{obs} vs. $[I]_0$ plots derived from the classical rate equation Eqn (1) are often very similar to k_{obs} vs. $[I]_0$ plots derived from Eqn (4). Thus, many enzymologists involved in drug-discovery research may have encountered nearly linear k_{obs} plots that (i) do not go through origin but instead intersect the Y-axis below the zero point; and (ii) are concave upward, or even show a distinct minimum, at low inhibitor concentrations instead of appearing either linear or hyperbolic (concave downward). As we can see from *Figure 1*, both of these qualitative characteristics are clear hallmarks of tight-binding (inhibitor depletion) actually occurring in the assay.

3. Results

This section presents the results of a heuristic simulation study that was designed to further illuminate the behavior of the tight-binding inhibition model and gain a practical experience in handing k_{obs} values derived under tight-binding experimental conditions. The numerical simulations were performed by using the software package DynaFit [6, 7]. All algebraic computations data fitting procedures were also independently verified by using the software package GraphPad Prism version 9.1 (GraphPad Software, San Diego, California USA, www.graphpad.com). The GraphPad Prism files, including the embedded user-defined fitting equations, are made available as part of the *Supporting Information* attached digitally to this report.

3.1. Simulated "tight-binding" data set

A collection of enzyme inhibition progress curves was simulated by according to the fully general first-order ordinary differential equation (ODE) formalism, using the software package DynaFit [6, 7]. The assumed kinetic mechanism is shown in the scheme below. The corresponding ODE system is shown in Eqns (8)–(12).

$$\begin{array}{ccccc} & & & \rightarrow & \leftarrow \\ E + S & \rightarrow & E + P & : & k_{sub} \\ E + I & \rightleftharpoons & E.I & : & k_{on} \quad k_{off} \end{array}$$
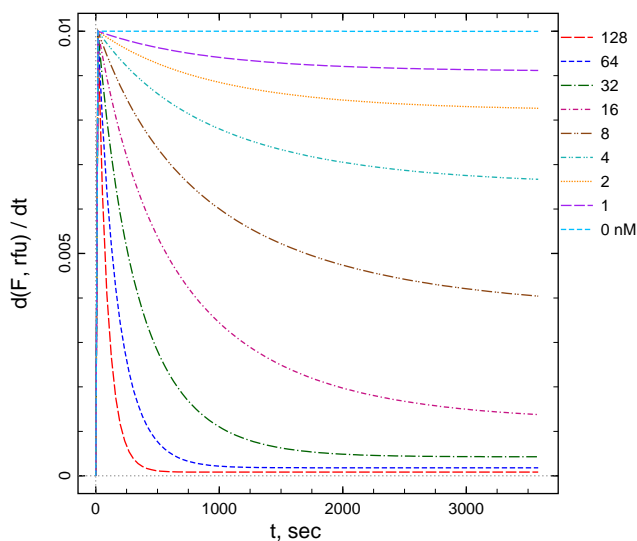
$$\frac{d[E]}{dt} = -k_{on}[E][I] + k_{off}[E.I] \qquad (8)$$

$$\frac{d[S]}{dt} = -k_{sub}[E][S] \qquad (9)$$

$$\frac{d[P]}{dt} = +k_{sub}[E][S] \qquad (10)$$

$$\frac{d[I]}{dt} = -k_{on}[E][I] + k_{off}[E.I] \qquad (11)$$

$$\frac{d[E.I]}{dt} = +k_{on}[E][I] - k_{off}[E.I] \qquad (12)$$

The simulated concentrations were $[E]_0 = 10$ nM, $[S]_0 = 10$ μM, and $[I]_0 = 128, 64, 32, 16, 8, 4, 2, 1, 0$ nM. The simulated

Figure 2: Simulated instantaneous reaction rates according to the one-step inhibition Mechanism **A**. Note that the instantaneous rate at zero inhibitor concentration is strictly constant, which justifies the application of Eqn (4). For further details see text.

rate constant values were $k_{sub} = 0.00001 \ \mu M^{-1} s^{-1}$, $k_{on} = 0.1 \ \mu M^{-1} s^{-1}$, and $k_{off} = 0.0001 \ s^{-1}$. Thus the equilibrium dissociation constant of the enzyme–inhibitor complex $K_i = k_{off}/k_{on} = 1$ nM, which is ten times lower than the enzyme concentration. Also note that approximately one half of the inhibitor concentrations are lower than the enzyme concentration (tight-binding). Altogether 60 data points were simulated for each progress curve spanning from time zero to $t = 3600$ s, or one hour. The normally distributed random experimental noise added to each data point had standard deviation equal to 0.7 percent of the maximum signal.

The instantaneous reaction rates associated with the simulated progress curves are shown in *Figure 2*. Note that, importantly, the reaction rate simulated at zero inhibitor concentration is unchanging, which means that the reaction progress curve simulated in the absence of inhibitors is strictly linear. This fully justifies the assumptions inherent in the integrated rate equation Eqn (4). Also note that at least several of the relatively high inhibitor concentration curves did reach a steady-state rate, which means that the simulated data set should contain sufficient inhibition to determine the reversible binding affinity.

3.2. Local fit of individual progress curves

All simulated reaction progress curves, except the positive control curve simulated at $[I]_0 = 0$, were fit separately to Eqn (4) to determine the best-fit values of the four adjustable model parameters v_0, v_i, k_{obs}, and F_0. In these regression analyses the enzyme concentration was held fixed at the nominal value $[E]_0 = 10$ nM. The results of fit are summarized graphically in *Figure 3*. The best-fit values of the apparent inhibition constant

k_{obs} and the associated formal standard errors (SE) are shown in *Table 1*.
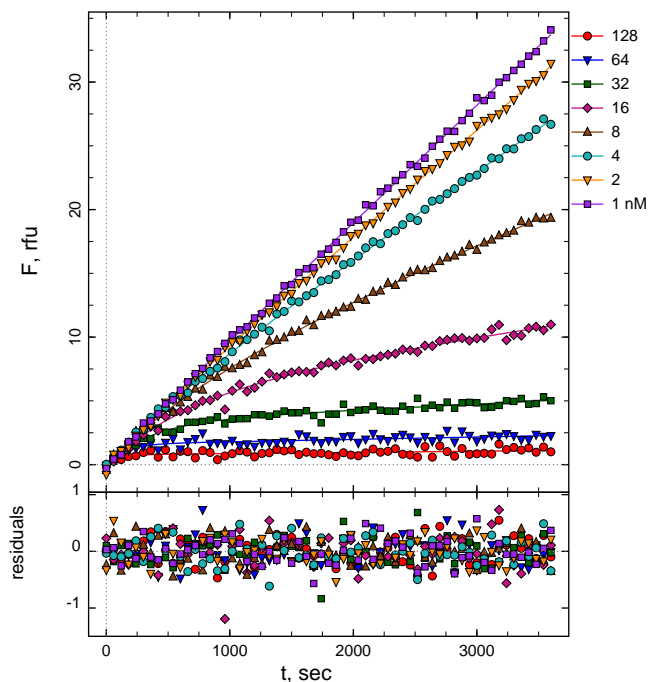
Figure 3: The results of fit of individual progress curves to the integrated rate Eqn (4). The results of fit to the alternate Eqn (1) were virtually indistinguishable, in that the residuals of fit (bottom panel) also appeared completely random.

	$1000 \times k_{obs}$, s^{-1}	
$[I]_0$, nM	from Eqn (4)	from Eqn (1)
128	10.50 ± 5.57	10.68 ± 5.63
64	6.78 ± 2.05	7.08 ± 2.11
32	2.61 ± 0.37	2.91 ± 0.38
16	1.11 ± 0.21	1.52 ± 0.22
8	0.87 ± 0.16	1.27 ± 0.19
4	1.00 ± 0.32	1.17 ± 0.36
2	1.69 ± 0.29	2.17 ± 0.66
1	2.16 ± 0.53	2.90 ± 1.47

Table 1: Best-fit values of k_{obs} from the fit of individual reaction progress curves depicted in *Figure 3*. The "±" values are formal standard errors from (unweighted) nonlinear regression analysis.

Table 1 purposely lists k_{obs} values determined both by the fit of reaction progress data to Eqn (4) and also by the fit of the same progress curve data to Eqn (1). Note that the best-fit values of are very similar to each other. A major practical significance of this result lies in that Eqn (4) as the fitting model is exquisitely sensitive to the initial estimate of model parameters v_0, v_i and k_{obs}. Therefore it proved very beneficial to always

perform all progress curve fits first to the classical rate Eqn (1) and then re-use the best-fit values of v_0, v_i and k_{obs} so obtained as initial estimates in the fit to Eqn (4).

Note that formal standard errors of k_{obs} results listed in *Table 1* vary by more then an order of magnitude. Thus in the subsequent analysis of the k_{obs} values it was crucially important to utilize *weighted least-squares fit*, with weighting factors set to the reciprocal squared standard error of each individual k_{obs} measurement, as opposed relying on the usual unweighted or ordinary least-squares (OLS) fit.

3.3. Fit of k_{obs} values to Eqn (6)

The results of weighted least-squares fit of the k_{obs} values listed in the second column of *Table 1* to Eqn (6) are shown graphically in *Figure 4*. Both rate constants k_{on} and k_{off} as well as the enzyme concentration $[E]_0$ were treated as adjustable model parameters. Non-symmetrical confidence intervals, at the 95% likelihood level, were computed according to the profile-t method of Bates & Watts [8, 9]. The numerical results are summarized in *Table 2*.
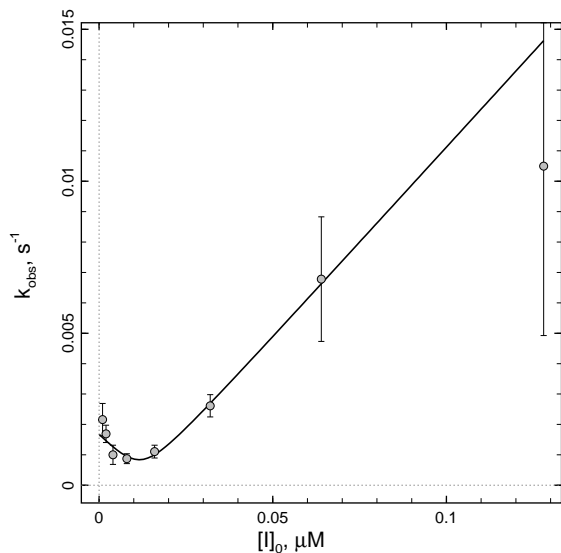
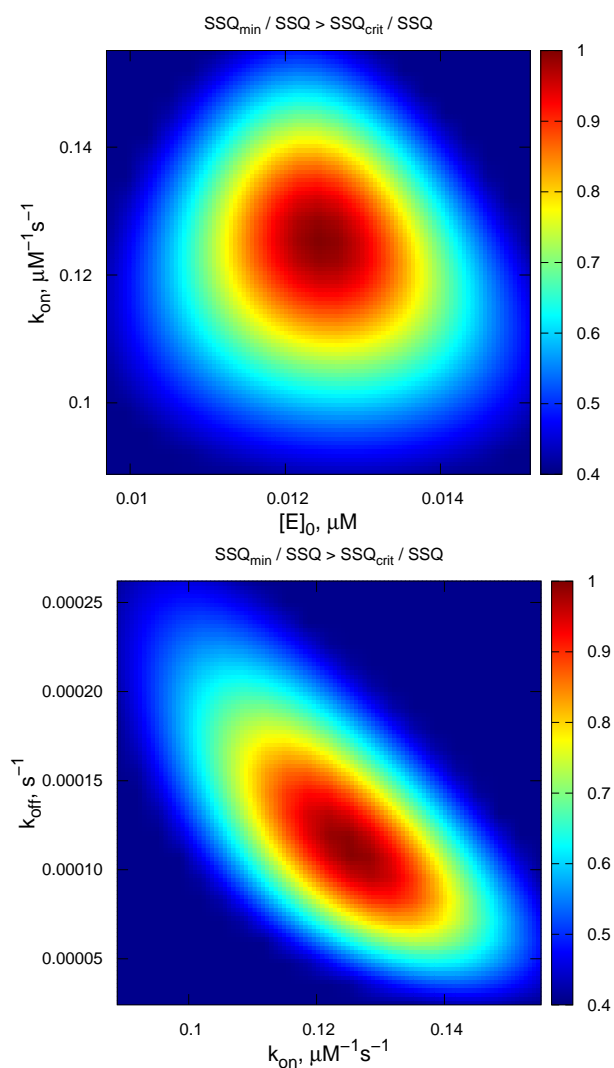**Figure 4:** Results of weighted least-squares fit of k_{obs} values listed in *Table 1* to Eqn (6).

parameter	best-fit $\pm$ SE	low $_{95\%}$	high $_{95\%}$
$[E]_0$, nM	12.5 $\pm$ 1.0	9.7	15.4
k_{on}, $\mu M^{-1}s^{-1}$	0.125 $\pm$ 0.013	0.089	0.158
k_{off}, msec^{-1}	0.11 $\pm$ 0.05	0.02	0.27

Table 2: Results of weighted least-squares fit of k_{obs} values listed in *Table 1* to Eqn (6). For details see text.

The results listed in *Table 2* show that the best-fit values of all three adjustable model parameters are in reasonably good agreement with the "true" (i.e., simulated) values. In particular, the best-fit value of the active enzyme concentration is $[E]_0 = 12.5$ nM, while the simulated "true" value was 10 nM,

representing an agreement within 25% systematic error. Very similar results were obtained for the association rate constant k_{on} (simulated "true" value 0.1 $\mu M^{-1}s^{-1}$, best-fit value 0.125 $\mu M^{-1}s^{-1}$). The best-fit value of the dissociation rate constant k_{off} agrees with the "true" value within 10%, but also note that the non-symmetrical confidence interval is approximately one order of magnitude wide (from 0.02 to 0.27 msec^{-1}).

As expected from the theoretical analysis presented above, the best-fit model curve depicted in *Figure 4* is neither linear nor hyperbolic, as could be expected in the absence of tight-binding, but rather it has a characteristic "field-hockey stick" shape, with a distinct minimum appearing near $[I]_0 \approx [E]_0 = 0.01$ μM. The slope of the nearly linear upward branch of the best-fit curve is equal to approximately 0.1 $\mu M^{-1}s^{-1}$, which is identical to the "true" value of k_{on}. The intercept on the k_{obs} axis is near $k_{obs} = 0.0017$ s^{-1}, which is approximately equal to the best-fit value of $k_{off} + [E]_0 k_{on} = 0.00011 + 0.0125 \times 0.125$ in appropriate units.

Figure 5: Joint confidence regions (95% likelihood level) of model parameters obtained in the weighted least-squares fit of k_{obs} values listed in *Table 1* to Eqn (6).

The joint confidence regions of adjustable model parameters are shown in *Figure 5*. Note that the enzyme concentration shows very little correlation with the rate constants, which is seen in very nearly circular joint confidence region in the upper panel of *Figure 5*. In contrast, the best-fit values of two rate constants k_{on} and k_{off} appear quite strongly correlated, which is seen in the ellipsoid shape of their joint confidence region.

4. Discussion

The kinetic behavior of enzyme inhibitors under tight-binding experimental conditions [2, 3] presents a special set of challenges to enzymology researchers, in particular those who are involved in drug discovery. The literature on the subject is often potentially confusing to the uninitiated.

For example, a well known textbook [1] first presents *both* the the classical integrated rate Eqn (1) *and* the tight-binding rate Eqn (4) in an introductory section entitled "Determining k_{obs}: The Rate Constant for Onset of Inhibition". Here the reader is correctly informed that in the absence of tight-binding we are allowed to use the simpler Eqn (1) to determine k_{obs} values, whereas in the presence of tight-binding we must use the more complex Eqn (4). In a subsequent section, entitled "Determination of Mechanism and Assessment of True Affinity", the book then proceeds to discuss how to differentiate between the one-step Mechanism **A** and the two-step Mechanism **B** based on the concentration dependence (linear or hyperbolic) of k_{obs} values. Unfortunately, this particular choice of sequencing the mathematical material can create a false impression among some readers that k_{obs} values determined *either* from Eqn (1) *or* from Eqn (4) can be used for mechanism discrimination in this particular manner. In fact, over the years, this investigator has encountered several internal reports and slide presentations, circulating inside various drug discovery establishments, where just such a misconception existed after exposure to the textbook in question [1]. One major motivation for the present report was to present a clarification of this complex mathematical issue.

To this end, let us try to uncover a possible origin of the generally confusing state of affairs. We can conveniently begin by reviewing a classic paper by Cha [4], where the mechanism selection Eqns (2)–(3) were first derived, alongside the newly derived Eqn (1). In a section of the paper entitled *Determination of k_{obs} and differentiation of mechanism*, Cha [4] lists Eqns (2)–(3) in his Table 1 on p. 2182 of the paper, and associates those two equations with Mechanism **A** and **B**, respectively. Then the author issues a crucially important caveat: "It must be pointed out that the significance of k_{obs} [...] holds true only when the depletion of free inhibitor by binding is negligible. Therefore, for this approach to be valid, the enzyme concentration must be an order of magnitude or more lower than the inhibitor concentration", meaning lower than even the lowest inhibitor concentration utilized in the inhibition assay. One major source confusion stems from the fact that Cha's paper is happens to be entitled "Tight binding inhibitors: I. Kinetic behavior". It is probably somewhat easy to lose track of the fact that many

results presented in Cha's 1975 paper do not actually apply to the tight-binding situation.

We can then proceed to another classic paper by Williams *et al.* [5], where the tight-binding of version of Cha's integrated rate Eqn (1) was first derived as Eqn (4). The authors state very clearly at the beginning of section *Theory and Data Analysis* that their newly derived rate Eqn (4) applies only to Mechanism **A**. They also add the following comment: "A more complex mechanism which predicts the slow development of inhibition is Mechanism **B** [...]. In this model an enzyme-inhibitor (EI) complex, which is formed rapidly, undergoes a slow isomerization to a second (EI*) complex. Attempts to derive an integrated equation for Mechanism **B**, analogous to Eqn (4), were unsuccessful [...] [T]he attempted solution leads to hopelessly complex algebra and an alternative technique must be sought. For particular values of the various parameters, the equations may be solved by *numerical integration*." Williams *et al.* [5] essentially state that they attempted but failed to derive a closed-form integrated rate equation that would apply to Mechanism **B** under tight-binding experimental conditions.

5. Summary and Conclusions

The tight-binding variant of the integrated rate Eqn (4) (shown as Eqn 6.2 in Copeland [1] and elsewhere in the biochemical literature) applies only to the one-step Mechanism **A**. Specifically, Eqn (4) does *not* apply to the two-step inhibition Mechanism **B**. Therefore, no attempts should be made to interpret k_{obs} values derived from Eqn (4) by using the classical (as opposed to tight binding) mechanism-selection formulas.

The overall shape of the k_{obs} vs. $[I]_0$ plot under tight-binding experimental conditions is neither linear nor hyperbolic, as is always the case in the absence of inhibitor depletion. Instead, the tight-binding k_{obs} plot has a relatively complex shape, generally concave upward, in many cases even including a local minimum. If inhibitor depletion is in fact prominent, the k_{obs} vs. $[I]_0$ data actually includes information about the concentration of the enzyme active sites.

Enzymology researchers involved in drug discovery, if and when actually using the "k_{obs}" method, should pay close attention the overall shape of k_{obs} plot. Any such plots that show local minima near $[I]_0 \approx [E]_0$ strongly indicate the actual presence of tight-binding in the assay. If so, Eqn (6) rather than the usual classical formulas should be used to interpret the k_{obs} results.

Acknowledgements

Supporting Information Available

GraphPad Prism data files utilized in this report, as compressed archive *GraphPad.zip*.

References

[1] R. A. Copeland, Evaluation of Enzyme Inhibitors in Drug Discovery, 2nd Edition, John Wiley, New York, 2013.

[2] J. F. Morrison, Kinetics of the reversible inhibition of enzyme-catalysed reactions by tight-binding inhibitors, Biochim. Biophys. Acta 185 (1969) 269–286.
URL http://bit.ly/3dOThIO

[3] J. W. Williams, J. F. Morrison, The kinetics of reversible tight-binding inhibition, Meth. Enzymol. 63 (1979) 437–467.
URL http://bit.ly/3Tafn8U

[4] S. Cha, Tight-binding inhibitors. I. Kinetic behavior, Biochem. Pharmacol. 24 (1975) 2177–2185.
URL http://bit.ly/3QNIWvw

[5] J. W. Williams, J. F. Morrison, R. G. Duggleby, Methotrexate, a high-affinity pseudosubstrate of dihydrofolate reductase, Biochemistry 18 (1979) 2567–73.
URL http://doi.org/10.1021/bi00579a021

[6] P. Kuzmič, Program DYNAFIT for the analysis of enzyme kinetic data: Application to HIV proteinase, Anal. Biochem. 237 (1996) 260–273.
URL http://doi.org/10.1006/abio.1996.0238

[7] P. Kuzmič, DynaFit - A software package for enzymology, Meth. Enzymol. 467 (2009) 247–280.
URL http://bit.ly/3R6jkJO

[8] D. M. Bates, D. G. Watts, Nonlinear Regression Analysis and its Applications, Wiley, New York, 1988.

[9] D. G. Watts, Parameter estimation from nonlinear models, Meth. Enzymol. 240 (1994) 24–36.
URL http://bit.ly/3CrSveY